Nitrogen Monoxide Interaction with Cu(I) Sites in Zeolites X and Y: Quantum Chemical Calculations and IR Studies

5 AUTHORS, INCLUDING:

Pawel Rejmak
Polish Academy of Sciences
10 PUBLICATIONS   105 CITATIONS

SEE PROFILE

Ewa Broclawik
Polish Academy of Sciences
154 PUBLICATIONS   1,466 CITATIONS

SEE PROFILE

Kinga Góra-Marek
Jagiellonian University
72 PUBLICATIONS   508 CITATIONS

SEE PROFILE

Nitrogen Monoxide Interaction with Cu(I) Sites in Zeolites X and Y: Quantum Chemical Calculations and IR Studies

Pawel Rejmak and Ewa Broclawik*

*Institute of Catalysis and Surface Chemistry, Polish Academy of Sciences, Niezapominajek 8,
30-239 Krakow, Poland*

Kinga Góra-Marek, Mariusz Radoń, and Jerzy Datka

Faculty of Chemistry, Jagiellonian University, Ingardena 3, 30-060 Krakow, Poland

The NO molecules adsorbed on Cu(I) sites in FAU lattice show strong red shift of stretching bond frequencies in comparison to the gas-phase NO. Three IR mononitrosyl bands can be found in Cu(I)Y (1815, 1793, and 1780 cm^{-1}) and two in Cu(I)X (1772 and 1757 cm^{-1}), respectively. Theoretical models allow association of all these bands with the species adsorbed on site II. The highest band in Cu(I)Y (1815 cm^{-1}), not observed in this work, is assigned to mononitrosyl species inside 6T rings with 1Al and Cu(I) coordinated to a single tetrahedron; the middle one (1793 cm^{-1}) derives both from 6T/1Al rings with 2(2) coordination and from 6T/2Al rings with 2(1) coordination, while the lowest band (1780 cm^{-1}) is due to the 6T/2Al rings with copper bound with two framework tetrahedrons. As for Cu(I)X, the higher (1772 cm^{-1}) and the lower (1757 cm^{-1}) bands are assigned to the adsorption complexes inside 6T/3Al rings with 2(1) and 3(3) coordination, respectively. No experimental mononitrosyl band is assigned to the species in site III, which may be populated by Cu(I) ions in Cu(I)X. This results from easier formation of dinitrosyls in this site, due to its better accessibility for the adsorbing molecules and slightly higher heat of the second NO adsorption. Dinitrosyls bands, about 1720 and 1820 cm^{-1} for Cu(I)Y and 1700 and 1820 cm^{-1} for Cu(I)X, do not show clear site specificity. Cu(I) in site II binds NO molecule much weaker than it does in site III. It is due to very stable planar 3-fold coordination to the framework O atoms, which is achieved in site II. The heats of the second NO molecule adsorption are only slightly higher at site III than at site II. This is because upon first NO molecule adsorption on site II, Cu(I) ions are displaced to the position more resembling site III. Low heat of adsorption may be regarded as one of the reasons responsible for lower Cu(I)FAU activity in the direct decomposition of NO in comparison to Cu(I)MFI.

1. Introduction

Copper-exchanged zeolites attract attention as promising catalysts and sorbents. Particularly they are known for their excellent catalytic properties in deNOx processes, both in the direct decomposition of nitrogen oxides[1,2] and in selective catalytic reduction with hydrocarbons[2,3] or ammonia.[4] Copper-exchanged faujasite (FAU) has been industrially applied recently in the latter process.[5] Other possible applications of Cu-FAU include synthesis of dimethyl carbonate[6] and selective adsorption.[7] Comprehensive review of present and perspective applications of Cu-exchanged FAU can be found in ref 5.

The deNOx processes on Cu-exchanged zeolites are generally considered as a redox reaction, with species containing monovalent Cu cations playing a crucial role.[8–11] Previous IR measurements showed NO stretching bond frequencies in Cu(I)-zeolites in the range 1790–1820 cm^{-1}[18–19] (see ref 20 for review), in comparison to 1876 cm^{-1} for the gas-phase molecule. NO activation by Cu(I) sites has been confirmed by theoretical studies, employing either small cluster models[16,21–27] or combined quantum mechanics/molecular mechanics (QM/MM) models.[28] It has been shown that weakening of the NO bond is caused by electron donation from Cu d orbitals to the antibonding SOMO in the NO molecule.[16,21,28] The interaction of the

Cu(I) ions with zeolitic O atoms is crucial for such a charge transfer mechanism: the cation is partly neutralized, while Pauli repulsion between Cu 3d orbitals and nonbonding orbitals on O atoms increases 3d orbital energy facilitating charge transfer from the cation to the ligand.[28] In contrast, in the gas-phase Cu(I)−NO complex, where donation from NO to the cation strongly prevails, depopulation of the antibonding NO π-orbital strengthens the NO bond.

The purpose of this work is the characterization of interactions between NO molecules and Cu(I) centers in FAU by combining infrared (IR) experiment and theoretical modeling. Investigation of NO adsorption is a necessary step in understanding all the consecutive processes that NO molecules undergo within zeolites and in explaining differences in deNOx behavior of various zeolitic systems. From among two main types of FAU zeolites, zeolite Y with Si/Al about 3:1 and zeolite X with Si/Al close to 1:1, a few IR measurements concerning adsorbed NO molecules on Cu(I)Y are known in the literature.[9,19] Additionally, IR studies on nitrosyl species in Cu(I)-exchanged ultrastable Y zeolite (USY) with Si/Al = 40:1 have been reported.[14] These data are somehow ambiguous due to the different methods of preparation of the samples and experimental conditions. The fact that the NO molecule is able to interact with both mono- and divalent Cu species and easily form dinitrosyl species multiplies difficulties in interpretation. Therefore theoretical

---

* Corresponding author. E-mail: broclawi@chemia.uj.edu.pl.

NO Interaction with Cu(I) Sites in Zeolites X and Y

J. Phys. Chem. C, Vol. 112, No. 46, 2008 **17999**

modeling can greatly contribute to the clarification of experimental results. Previous computational studies on nitrosyl species in Cu(I)-zeolites deal mostly with small cluster models,[16,21–27] which, although they give valuable insight into the nature of interaction between NO and Cu(I)-zeolite systems, are hardly able to describe differences between various zeolitic matrices or different ionic sites within given lattice type. More elaborate QM/MM methods have been applied so far only to the mononitrosyl species inside the high-silica MFI and ferrierite (FER) zeolites.[28] Our work combines new IR data, obtained for both main types of FAU, namely, Y zeolite and X zeolite, with theoretical results from QM/MM calculations for FAU models with different Al loadings. Both IR results for NO−Cu(I)X zeolite and the application of hybrid QM/MM approach for NO−Cu(I)FAU models are, up to our best knowledge, the first ones presented in the literature.

2. Experimental Procedures

Zeolites CuX and CuY were prepared from a parent NaX and NaY forms, respectively, by the ion exchange from the solution of $Cu(CH_3COO)_2$. The exchange degrees were 80% and 60% for CuX and CuY, respectively. Si/Al ratio is 1.3 for X zeolite and 2.5 for Y zeolite. Prior to IR experiments, the samples CuX and CuY were activated in an IR cell at 720 K at vacuum. The Cu(II) ions, which survived the self-reduction to Cu(I) during the pretreatment at vacuum, were reduced to Cu(I) cations by the reaction with formaldehyde. Reduction was performed at 370 K. Gaseous formaldehyde was obtained by heating (at ca. 370 K) paraldehyde (Aldrich). Doses of NO were adsorbed at 150 K to avoid the partial reoxidation of Cu(I) to Cu(II) with pressures spanning from 0.1 to 50 Torr. The IR spectra were recorded using Eqinox 55 spectrometer (BRUKER) equipped with MCT detector at spectral resolution 2 cm^{-1}.

3. Computational Procedures

3.1. Methods. The combined quantum mechanics/interatomic potential functions method (QMPot)[29,30] is applied to describe interactions between Cu(I)FAU and one or two NO molecules. Within this approach, the periodic system is divided into the cluster, containing the active center and adsorbing molecules, described by accurate QM methods, and the rest of the lattice treated in an approximate way by less computationally expensive MM methods. QMPot has been proven as a very convenient approach in the description of zeolitic systems, giving more reliable results than free cluster models and with shorter computational time than periodic full QM modeling.[31] Calculations are performed with the QMPOT program[30] coupling the Turbomole suite[32] at the QM level with the GULP package[33] at the MM level. Shell-model ion-pair potential[34] is used in the MM part with parameters for from refs 35 and 36. Short-range interactions between the NO molecule and framework O atoms are described by Lennard-Jones potential with parameters from Universal Force Field.[37] Interactions of Cu−NO and NO−NO are described only at the QM level. Density functional theory (DFT) with the PBE exchange−correlation functional[38] and the TZVP basis set[39] is applied in the QM part. In selected cases, the B3LYP functional[40] is also employed. The MARI-J approximation[41] is used to accelerate the DFT calculations. In view of qualitative discrepancies between B3LYP and PBE descriptions of dinitrosyl species, benchmark calculations using high-level *ab initio* methods are invoked in order to investigate the reliability of the DFT method in this case. With this aim, complete active space self-consistent field second-order perturbation theory (CASSCF/CASPT2)[42] and Møller−Plesset second-
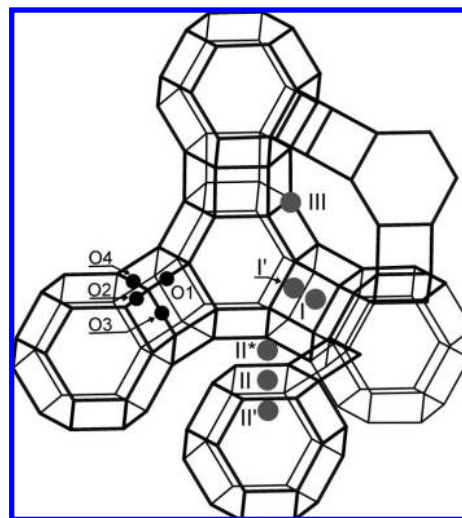

Figure 1. Possible cation sites (gray balls) and different crystallographic O atom positions (black balls).

order perturbation theory (MP2) calculations are performed for simplified models, using Molcas 6.4/7.0 suite[43] with standard settings (IPEA-shifted zero-order Hamiltonian, an imaginary level shift of 0.1 hartree, and scalar relativistic effects included via Douglas−Kroll−Hess second-order transformation[44]). Atomic natural orbitals (ANO) are used as the basis set, with ANO-RCC basis[45] for Cu and Al atoms (contracted to 7s6p5d2f1g for Cu and to 5s4p2d for Al) and ANO-S basis[46] for other atoms (contracted to 4s3p1d for N and O and to 2s for H). The choice of the active orbitals will be discussed under the Results section. For technical reasons, all MP2 calculations were performed using the CASPT2 module, with CASSCF reference corresponding to Hartree−Fock configuration (i.e., no active orbitals for the closed shell systems or one singly occupied active orbital for the open shell ones).

3.2. Models. FAU crystallizes in the *Fd*3*m* framework type. The cubic lattice unit cell consists of 192 Si or Al atoms and 384 O atoms. Si and Al atoms will be called "T atoms", due to their tetrahedral coordination by framework O atoms. For the sake of brevity, we denote structural units in the lattice or QM clusters consisting of *n* T atoms as *n*T cluster/unit, depicting the number of Al atoms as *n*T/*m*Al species. For computational convenience, we apply a smaller rhombohedral unit cell with only 48 T and 96 O atoms. Only one crystallographic position of the T atom and four different O atom positions are present. The FAU lattice consists of cubooctahedral units, called sodalite units, connected by hexagonal prisms (Figure 1). This system of sodalite units and hexagonal prisms surrounds a large empty cavity, called a supercage, which can be easily penetrated by adsorbing molecules. Excess framework negative charge upon substition of Si(IV) by Al(III) is compensated by the extraframework cations. Three main cationic sites are distinguished:[47] site I inside the hexagonal prism, inaccessible for molecules; site II close to the plane of the 6T ring, and site III above 4T rings in the wall of the supercage. Each site has some subspecies, distorted from "pure" site geometry, and some authors use different notation. Diffraction experiments for Cu(I)Y show monovalent copper cations occupying site I′ (inside the hexagonal prism, close to its base) and some subspecies of site II.[19,48] Previous QMPot studies[49] have confirmed that the most stable Cu(I) sites are those with planar trigonal coordination to framework O atoms, which can be achieved in the plane of 6T rings, either in the bases of hexagonal prisms (site I′) or in the walls of supercages (site II). Site III with 2-fold
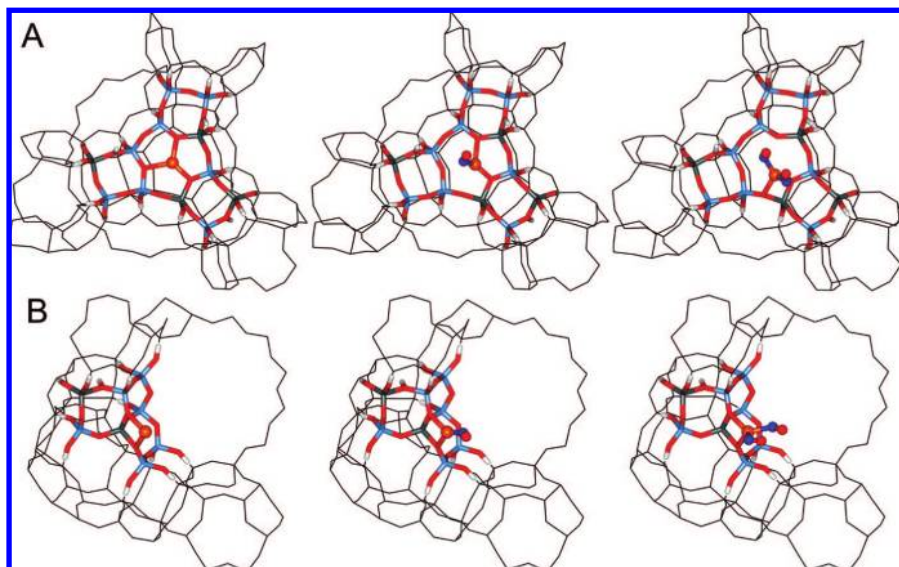
Figure 2. Cu(I) sites in FAU zeolite and NO adsorption systems, fragments of the optimized QMPot structures: from left to right, Cu(I) centers alone and monitrosyl and dinitrosyl complexes on site II (Y model with 6T/2Al-*meta* ring) and on site III (Y model with two Al atoms). QM clusters are depicted with sticks and Cu(I) ions and NO molecules with balls.

coordination is much less stable, which explains the lack of occupation of this site in Cu(I)Y. However, this site may become populated at high Cu(I) loading in high-alumina zeolite X or in the presence of some cocations, preferably occupying sites I′ or II instead Cu(I). Sites I′, hosting about one-half of the Cu(I) ions,[19] are not accessible for the adsorbing molecules, thus they will not be further considered in the present study.

The construction of the QMPot geometric model consists of two steps: choosing the periodic lattice model for the MM part, and then cutting off the cluster model subjected to QM calculations. The initial structures are taken from experimental data.[50] Unit cell parameters ($a = 17.4931$, $b = 17.4300$, $c = 17.4855$ Å, $\alpha = 59.898°$, $\beta = 59.870°$, $\gamma = 59.995°$) for constant volume QMPot optimizations have been taken from shell-model optimization of the $Si_{47}Al_1O_{96}H$ structure.[49] In all cases, Al distributions in all models satisfy the Loewenstein rule,[51] excluding Al−O−Al connectivities. If more than one Al atom is present in the lattice, protons are charge-compensating cocations. The simplest model, called the "high silica" (HS) model, assumes an almost pure silica lattice with up to a few Al atoms solely in the part of the lattice used to construct the QM cluster. However, in this case, the environment, being pure silica, is a rather poor model for high-alumina Y and X lattices. The HS model might be also treated as a model of ultra-high-stability Y zeolite (UHSY) with Si/Al = 40:1, though with some caution, stemming from the preparation of USY that may lead to significant distortion from the ideal FAU structure.

More reliable FAU models should consider the presence of Al atoms in the whole lattice. Some difficulties with constructing high-alumina QMPot models arise here. Having decided that Al charge-compensating species are, except one Cu(I) ion per unit cell, protons, we must distribute them within the model avoiding terminating −OH$_2$ groups in the QM cluster. Such termination would introduce some computational errors. Particularly it is hardly possible to construct a QMPot model of X zeolite with Si/Al ratio close to 1:1 and thus a large number of protons. Further, having fixed Al ion and proton distribution in the lattice, we find it difficult to construct QM clusters differing only by the number of Al atoms in the nearest neighborhood of the Cu(I) cation with the number of Al atoms in the background kept constant. Thus some differences in the results can be due

to the unbalanced treatment of Al loading in the QM and MM parts of various models. Last but not least, all high-alumina lattice models treated here are merely a few samples of the vast number of different Al distributions that can occur in nature.

The HS model and the Y1 model (unit cell composition $Si_{36}Al_{12}O_{96}CuH_{11}$) are identical to those used in ref 49. In addition, to construct QM clusters for site II differing only by the number of Al atoms within the 6T ring (i.e., the closest vicinity of Cu(I)) and having a fixed number of Al atoms in the outer part of clusters, the Y1 lattice has been modified, either by removing one Al atom ($Si_{37}Al_{11}O_{96}CuH_{11}$ unit cell composition) or by changing Al and H siting. We refer to such lattice models collectively as the "Y2 model". Thus site II QM clusters embedded in the Y2 lattice have one or two Al atoms in the 6T ring (closest Cu(I) neighborhood) and always one Al atom in the peripheral 4T ring (next neighborhood). To improve the description of high-alumina X zeolite, we use the unit cell with the composition $Si_{34}Al_{14}O_{96}CuH_{13}$ and locally increased density of aluminum. Such a lattice model allows construction of a QM cluster containing three Al atoms within the 6T ring (i.e., closest Cu(I) vicinity) and is referred to as the "X model".

For the description of sites II and III, clusters built of 12 T atoms (Figure 2A) or built of 8 T atoms (Figure 2B), respectively, are used in the QM part. In the HS lattice model, site II clusters contain one to three Al atoms, all within the 6T ring. In the case of two Al atoms in the 6T ring, two mutual Al orientations are possible, called *meta* for Al−Si−Al and *para* for Al−Si−Si−Al sequences, respectively. Site III clusters contain one to four Al atoms. In the Y1 lattice model, it is possible to construct two types of clusters for site II: either clusters having 6T/1Al and 6T/2Al-*meta* rings and an additional two Al atoms outside the 6T ring or clusters having a 6T/2Al-*para* ring and one Al atom outside the 6T ring. There are also site II clusters embedded in the Y2 lattice model with 6T/1Al, 6T/2Al-*meta*, and 6T/2Al-*para* rings and always one Al atom in the outer part of the cluster. In the zeolite X lattice model, site II is represented in the QM part by a cluster with a 6T/3Al ring and two Al atoms outside the 6T ring. We use also a site III cluster model with two Al atoms in the Y1 model.

Test calculations for site II 16T clusters show that further increase of the cluster size for this site does not change results.
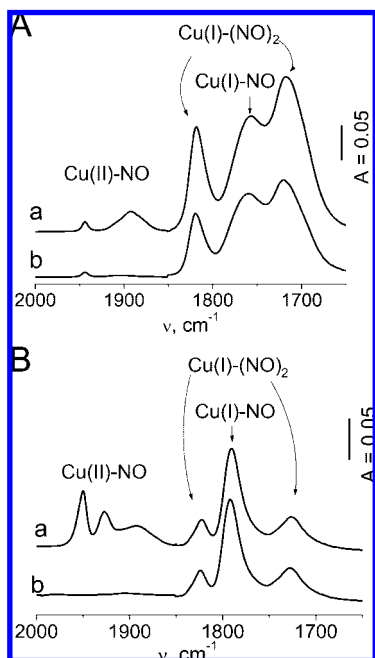
Figure 3. The spectra of NO interacting with Cu(I) and Cu(II) sites in zeolites CuX (A) and CuY (B). The spectra were recorded before (a) and after (b) the treatment with formaldehyde. All spectra were recorded upon saturation of all Cu(II) sites with NO.

However, for site III in some cases larger 20–22T clusters, embedded in double cell, are applied.

In order to evaluate the reliability of DFT methods for the studied systems, the simplified free cluster model of the adsorption complex, namely, $AlO_4-Cu(I)-(NO)_{0-2}$, is used in various benchmark *ab initio* calculations.

4. Results

4.1. Experimental Results. *Reduction of Cu(II) with Formaldehyde.* It is well-known that most Cu(II) ions present in Cu-zeolites are reduced to Cu(I) during the activation of zeolites at vacuum at temperatures above 600 K. However, as our previous studies[52] evidenced, some Cu(II) ions survived the activation. This is well seen by analyzing the spectra of sorbed NO, because the N–O stretching frequency is very sensitive to the valence state of Cu. The spectra of NO sorbed in CuX and CuY zeolites are presented in Figure 3A,B (spectra a). These spectra show the bands of Cu(I)–NO and Cu(II)–(NO)$_2$ adducts (1700–1850 cm^{-1}), as well as of Cu(II)–NO (1850–2000 cm^{-1}), indicating that zeolites CuX and CuY contain some non-reduced Cu(II) ions.

In order to reduce the remaining Cu(II) to Cu(I), reaction with formaldehyde was performed. Our earlier IR results[53] evidenced that formaldehyde was oxidized by Cu(II) to formate ions HCOO$^-$ and Cu(II) was reduced to Cu(I). The spectra of formaldehyde interacting with CuX zeolite are presented in Figure 4. Spectrum a, recorded upon the sorption of formaldehyde at room temperature, shows the bands of carbonyl group, 1712–1726 cm^{-1}, and the band of scissoring vibration of CH$_2$ group (1503 cm^{-1}). Heating to 370 K (spectrum b) results in the oxidation of formaldehyde to formate ions, which is accompanied by the substitution of the formaldehyde bands by the formate ions bands, symmetric and antisymmetric stretching modes of COO$^-$ (1694 and 1361 cm^{-1}), as well as C–H bending ones (1383 cm^{-1}). The formate ions were subsequently decomposed by evacuation at 720 K, which resulted in the vanishing of formate ion bands. A similar situation was also
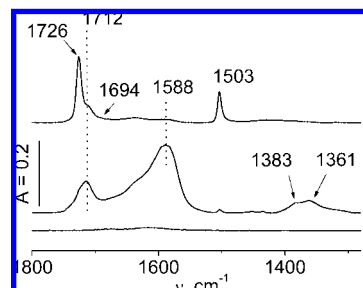

Figure 4. The spectra recorded upon the sorption of formaldehyde at room temperature in zeolite CuX (a), heating of zeolite with formaldehyde to 370 K (b), and evacuation at 720 K (c).
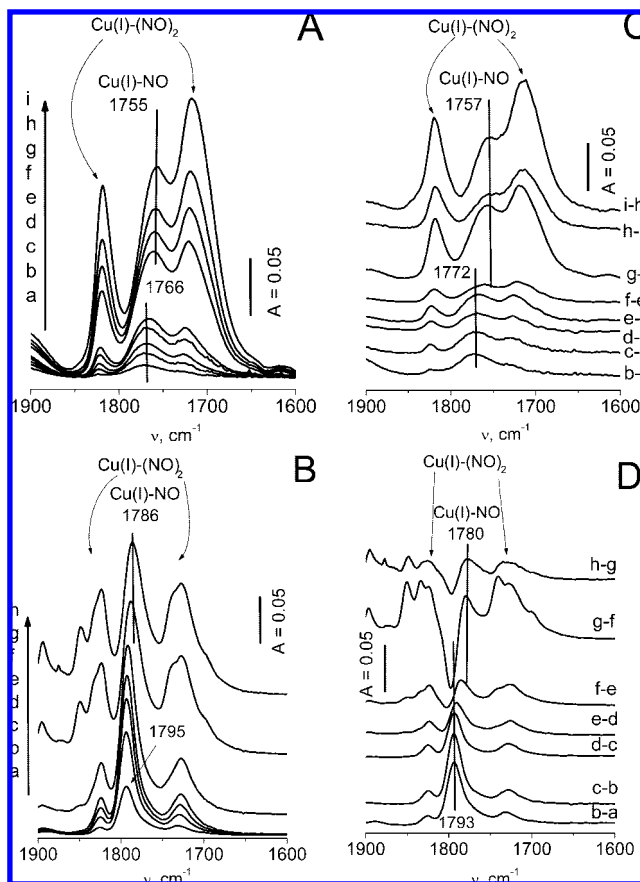

Figure 5. The spectra recorded upon the sorption at room temperature of increasing amounts of NO in zeolites CuX (A) and CuY (B), along with the difference spectra for CuX (C) and CuY (D). Small letters on panels A and B denote increasing dosage of NO. The notations *x-y* on panels C and D denote the difference between spectra recorded at the *y*th and *x*th NO dosage.

observed in the case of zeolite CuY (spectra not shown) and also in our earlier study on zeolite CuMFI.[53] The spectra of NO sorbed in zeolites CuX and CuY reduced with formaldehyde (Figure 3A,B, spectra b) show practically only the bands of Cu(I)–NO, indicating that almost all Cu(II) that survived the activation at vacuum at 720 K were reduced by formaldehyde to Cu(I).

Interaction of NO with Cu(I) Sites in Zeolites Cu(I)X and Cu(I)Y. The spectra of NO sorbed in zeolites CuX and CuY are presented in Figure 5A,B. At low coverage (spectra a) practically only the bands of Cu(I)–NO mononitrosyls (1766 cm^{-1} for CuX and 1795 cm^{-1} for CuY) are developed, while at higher coverages (spectra b–i) the bands of Cu(I)–(NO)$_2$ dinitrosyls (ca. 1720 and 1820 cm^{-1} in Cu(I)Y and 1700 and
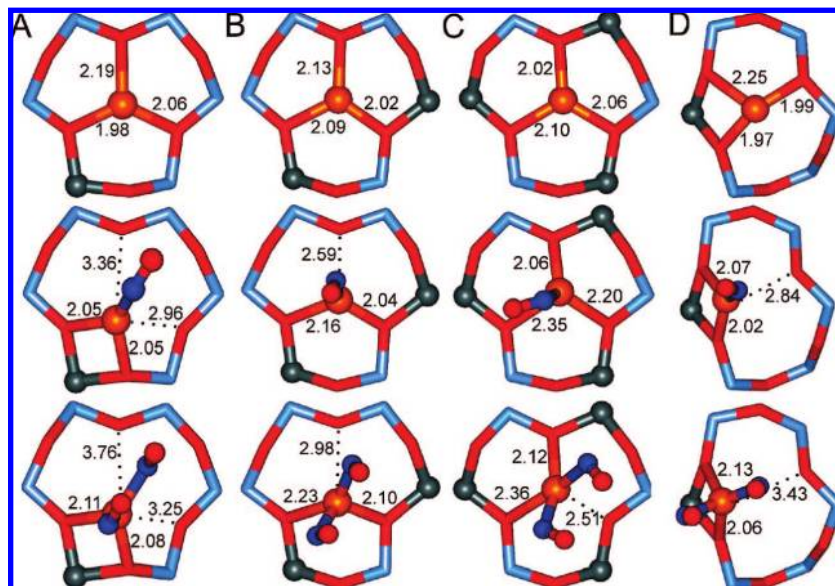
Figure 6. Cu(I) coordination before and after NO adsorption, the nearest Cu(I) neighborhood from optimized QMPot structures. Sites II in FAU: (A) 6T ring with one Al atom (HS model); (B) 6T ring with two Al atoms in *meta* position (Y2 model); (C) 6T ring with three Al atoms (X model). For comparison, site I in MFI (6T ring with one Al atom in T4 position) is shown in panel D. Mononitrosyls (A, C) are bent toward the plane of the 6T ring; that in panel B is bent from the 6T ring. Cu and Al atoms and NO molecules are depicted with balls. The most important Cu−O distances given in Å.

1820 cm^{-1} in Cu(I)X) grow with the amount of NO sorbed. Both for zeolite CuX and for zeolite CuY, the bands of mononitrosyls and dinitrosyls increase simultaneously with the amount of NO sorbed. Contrary to CuX and CuY, in zeolite CuZSM-5 the band of mononitrosyl grows first, and subsequently, at higher NO loadings, mononitrosyls are transformed into dinitrosyls.

The comparison of the spectra presented in Figure 5A,B shows that the Cu(I)−NO band shifts to lower frequencies with NO loading. More information on the nature of Cu(I)−NO adducts is obtained from the analysis of the difference spectra[54] presented in Figure 5C,D. These difference spectra show that both for Cu(I)X and for Cu(I)Y, two Cu(I)−NO bands are present: 1757 and 1772 cm^{-1} for Cu(I)X and 1780 and 1793 cm^{-1} for Cu(I)Y.

Difference spectra (Figure 5C,D) show also that for both Cu(I)X and Cu(I)Y, the sites represented by the higher frequency Cu(I)−NO band are occupied first, that is, at lower NO loadings. A similar situation was observed when CO was sorbed in zeolites Cu(I)X and Cu(I)Y: two Cu(I)−CO bands were observed, and the adducts of the high-frequency band appeared at lower CO loadings and desorbed at higher temperatures.[55] The results obtained in this study evidence the presence two bands of mononitrosyl species in zeolite Cu(I)X (Cu(I)−NO bands at 1757 and 1772 cm^{-1}). Two kinds of Cu(I) were also found in Cu(I)Y (Cu(I)−NO bands at 1780 and 1793 cm^{-1}). However, it should be noted that Turnes Palomino et al.[19] reported also (besides a 1792 cm^{-1} band) a Cu(I)−NO band at 1815 cm^{-1}. A band of similar frequency (1819 cm^{-1}) has been also reported in Cu(I)USY.[14] It may be concluded therefore that three bands of Cu(I) mononitrosyls, 1780, 1793, and 1815 cm^{-1}, exist in zeolite Cu(I)Y, whereas two mononitrosyl bands, 1757 and 1772 cm^{-1}, are found in zeolite Cu(I)X.

4.2. Computational Results. *Structural and Energetic Properties of Mononitrosyl Species.* The most stable Cu(I) sites are those with copper coordinated in-plane to three framework O atoms, belonging to three separate TO$_4$ units,[49] namely, sites I′ and II (similar to sites I* and II*, respectively, according to ref 19). Denoting Cu(I) coordination to the framework oxygen atoms as $m(n)$, where m is the number of coordinating O atoms and n is the number of distinct TO$_4$ units to which they belong, we refer to this coordination as 3(3). Site III with 2-fold coordination is much less stable. Subspecies with 2(1) coordination over the edge of two 4T rings (sometimes denoted as III′) are slightly more preferred than those with 2(2) coordination, adjacent to the plane of a single 4T ring ("pure" site III according to ref 47).

NO adsorption on site II is associated with a significant change in Cu(I) coordination. Interaction with the NO molecule withdraws the Cu(I) ion from the plane of the 6T ring toward the supercage and usually lowers its coordination to the framework O atoms. In the HS model in all cases, NO adsorption switches Cu(I) coordination from 3(3) to 2(1), that is, copper cation coordinated by two O atoms of a single AlO$_4$ (Figure 6A). Being bound that way to two zeolitic O atoms and the N atom of the ligand molecule, the copper cation maintains its total planar trigonal coordination. Only for site II with the 6T/3Al ring, adsorption complex with Cu(I) insignificantly displaced above the 6T ring plane and maintaining 3(3) coordination is additionally found, although the bond with the third O atom is strongly elongated. In this case, Cu(I) has a distorted tetrahedral coordination. In Y1 and Y2 models, apart from adsorption complexes with 2(1) copper coordination, species with 2(2) coordination are also found (Figure 6B). In this case, Cu(I) displacement above the 6T ring is smaller. Total Cu(I) coordination is again 3-fold d planar (two O atoms of two different TO$_4$ and N atoms). Nitrosyl species with 2(1) coordination are always present in 6T/1Al rings in addition to those with 2(2) coordination. In some models containing 6T/2Al rings, only nitrosyl complexes with 2(2) coordination occur. For 6T/3Al rings embedded in the Y lattice ("X model") again nitrosyl forms with 2(1) and 3(3) copper coordination are found simultaneously, just as in the 6T/3Al ring in the HS model (Figure 6C). NO adsorption on unsaturated Cu(I) in site III does not introduce major changes in the Cu(I) siting, namely, 2(1) or 2(2) coordination is maintained upon NO adsorption (Figure 7).
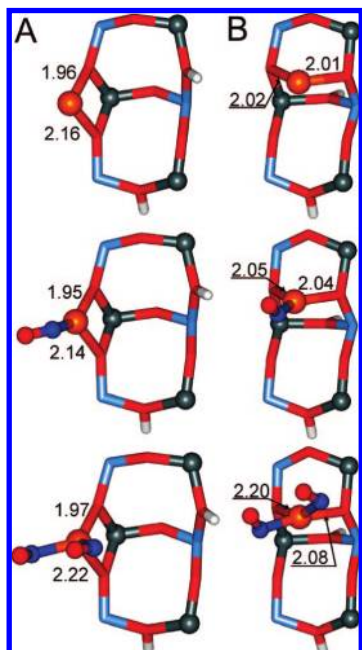
Figure 7. Cu(I) coordination before and upon the NO adsorption, QMPot structures. Sites III in FAU: (A) Cu(I) coordinated to single AlO$_4$ (HS model, 4Al-113); (B) Cu(I) coordinated to two AlO$_4$ units (HS model, 3Al-33). Cu and Al atoms and NO molecules are depicted with balls. The most important Cu–O distances given in Å.

Cu(I)–NO species always have angular structure. Angles are in the range 141°–147° for site II species with 2(1) copper coordination and site III, while they are in the range 133°–140° for site II with 2(2) and 3(3) coordination. In site II, both structures with Cu–N–O bent toward and out of the plane of the 6T ring are found. Cu–N bond lengths are about 1.80 Å for site II with 2(1) coordination, 1.83–1.85 Å for site II with higher Cu(I) coordination, and about 1.79 Å for site III. NO bond is elongated by about 0.15 Å in comparison to the gas-phase molecule (1.1596 Å from PBE/TZVP calculations). The details of structural results can be found in Supporting Information.

The adsorption energies of NO molecules are calculated as the energetic effect of the reaction

$$(NO)_{x-1}-Cu(I)FAU + NO_{gas} \rightarrow (NO)_x-Cu(I)FAU$$
$$x = 1, 2 \quad (1)$$
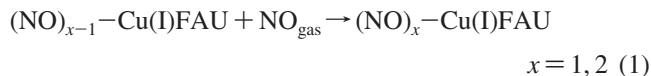
Deformation energies are defined as the difference between the energies of Cu(I)FAU structure without NO but in optimal geometry of $(NO)_{1-2}$–Cu(I)FAU species and optimal Cu(I)FAU structure.[28] We would like to underline that no kinetic modeling is performed in the present work. Some suggestions concerning the kinetics presented in the discussion are merely suggestions based on the comparison of relaxation degree of equilibrium structures and deformation energies. The latter ones by no means can be treated as the activation barrier. Actually it is not proven that NO adsorption is the activated process. However, it seems reasonable to assume that adsorption complexes with smaller relaxation of active sites may be formed faster.

It has already been reported that the PBE functional strongly overestimates the energies of binding a single ligand molecule by Cu(I)[56] while B3LYP gives values in fine agreement with experiment.[28] Therefore we have performed B3LYP calculations for selected models (listed below) to correct PBE energies by the ratio between basis set superposition error (BSSE)-corrected B3LYP and PBE values according to the formula

$$f = (E_{ads\_QMPot} + BSSE)_{B3LYP}/(E_{ads\_QMPot} + BSSE)_{PBE} \quad (2)$$

Assuming that this ratio is constant for given types of mononitrosyl species, scaled heats of adsorption at 0 K are calculated as

$$\Delta H_{ads} = f(-E_{ads} + BSSE)_{PBE} - \Delta ZPVE_{PBE} \quad (3)$$

Apart from additional B3LYP calculations, BSSE and zero-point vibrational energies (ZPVE) are calculated for selected structures from the HS model (site II with one and three Al, site III with protonated O1,O1 and O3 atoms) and the Y1 model (site II, 2Al-*meta*, and site III). BSSE is obtained using the counterpoise method.[57] BSSE corrections for the mononitrosyl species at the PBE level are in the range 8–11 kJ/mol and at the B3LYP level in the range 7–8 kJ/mol. For dinitrosyls, these corrections are 5–6 kJ/mol. The values of f calculated for HS–site II-1Al, HS–site II-3Al, and Y1–Al-*meta* models are 0.58, 0.43, and 0.48, respectively. The average value (0.48) is taken for the remaining site II models. For site III, f_{B3LYP} is 0.66. $\Delta ZPVE_{PBE}$ is the correction for zero-point vibrational analysis calculated in harmonic approximation at the QMPot/PBE level for solid reagents and at the QM level for gas-phase NO. ZPVE corrections at the PBE level are 6 kJ/mol for site III and 5 kJ/mol for site II ($\Delta ZPVE$ in different models varies in the range 4–6 kJ/mol). For dinitrosyls, B3LYP fails to predict the second NO binding at all, and therefore a scaling factor obtained in a different procedure has to be applied. Here, MP2 and CASPT2 calculations for simplified cluster models served as the reference level, leading to the scaling factor for PBE energies of 0.6 (*vide infra*). The influence of thermal contributions to the PBE enthalpy of adsorption has been also evaluated at 298 K. For solids, only vibrational contributions have been considered, while the translational, rotational, and vibrational contributions along with volume work in the ideal gas approximation have been taken into account for gas-phase NO ($-7/2RT$ in total). In agreement with the previous study on diatomic molecule adsorption,[28,49] the total thermal effect is found to be negligible (about +2 kJ/mol) and is not further included in presented values. Thus ΔH_{ads} should be the directly comparable to experiment. Interaction energies of the single NO molecule with Cu(I) are given in Tables 1 and 2.

A single NO molecule is bound more strongly by less stable Cu(I) sites, namely, site III, with the heats of adsorption about 105 kJ/mol for sites with 2(1) copper coordination and 85 kJ/mol for sites with 2(2) coordination. The heats of adsorption on site II are 2–3 times smaller. In the HS model, the decrease in NO binding with the number of Al atoms in the 6T ring is clearly seen, but this trend is not conserved in Y lattice models. For a specified site II type, mononitrosyl species with variable Cu(I)–O coordination have practically the same stability. However, for 6T/1–2Al rings, species with 2(1)-coordinated Cu(I) are slightly more stable, while in 6T/3Al rings, 3(3) coordination is slightly favored over 2(1) coordination with respect to NO binding. For given Cu(I) coordination, mononitrosyl complexes with NO bent "toward" and "out of" plane of the 6T ring are energetically equally stable.

Deformation energies are much larger for site II than for site III. For the latter, values are very small, being several kilojoules per mole for species with 2(1) and a dozen or so kilojoules per mole for those with 2(2) copper coordination. Site II deformation energies vary between 40 and 80 kJ/mol. In the HS model, site II with 6T/1Al and 6T/2Al rings, always achieving 2(1) copper coordination upon NO adsorption, have deformation energies mounting to about 75% of the absolute value of the energies of adsorption (60–70 kJ/mol). In Y models, deformation energies

TABLE 1: QMPot Results for HS MODEL, Energies of Adsorption (ΔE_{ads}), Deformation Energies (E_{def}), and Scaled Heats of Adsorption (ΔH_{ads}) in kJ/mol, N−O Distances (Å), Cu−N−O Angles (deg), and NO Bond Stretching Harmonic Frequencies (cm^{-1})

Cu(I) site	nAl−O(H)[a]	CN_{Cu}[b]	ΔE_{ads} (E_{def})[c]	ΔH_{ads}[d]	R_{N-O}	θ_{Cu-N-O}	ω_{NO}	$\langle\omega_{NO}\rangle$[e]
site II	1Al	2(1)	−108 (61)	52	1.175	143.6	1784 (1785)[f]	1788
					1.174	145.8*[g]	1792	
	2Al-*meta*-1[h]	2(1)	−96 (71)	37	1.177	143.0	1771	1776
					1.176	145.7*	1781	
	2Al-*para*-1	2(1)	−94 (73)	36	1.177	142.3	1768	1773
					1.176	145.8*	1778	
	3Al-1,1	2(1)	−81 (85)	26	1.180	142.2	1756	1762
					1.178	145.4*	1767	
		3(3)	−87 (44)	29	1.180	137.3	1746	1742
					1.181	136.4*	1738	
site III	1Al	2(1)	−176 (3)	104	1.176	145.8	1786	1786
	3Al-3,3	2(2)	−150 (12)	86	1.175	144.8	1786 (1800)	1786
	4Al-1,1,3	2(2)	−179 (3)	106	1.175	145.8	1783 (1805)	1783

^{a} nAl-m: n denotes number of Al atoms within the QM cluster; m are crystallographic types of protonated O atoms. ^{b} Cu coordination number to framework O atoms. $m(n)$: m denotes total Cu−O coordination number; n number of distinct coordinated TO$_4$ units. ^{c} See text for definition. ^{d} Calculated according to the eq 3. ^{e} See text for clarification. ^{f} Values in parenthesis obtained for larger QM clusters, 16T for site II and 22T for site III. ^{g} Star depicts Cu−N−O species bent toward the plane of 6T ring. ^{h} *Meta* and *para* denote mutual Al atom positions in 6T ring.

TABLE 2: QMPot Results for Selected Y and X Zeolite Models, Energies of Adsorption (ΔE_{ads}), Deformation Energies (E_{def}), Scaled Heats of Adsorption (ΔH_{ads}) in kJ/mol, N−O Distances (Å), Cu−N−O Angles (deg), and NO Bond Stretching Harmonic Frequencies (cm^{-1})

model		nAl[a]	CN_{Cu}[b]	ΔE_{ads} (E_{def})[c]	ΔH_{ads}[d]	R_{N-O}	θ_{Cu-N-O}	ω_{NO}	$\langle\omega_{NO}\rangle$[e]
Y1[f]	site II	1Al (2)	2(1)	−83 (79)	31	1.174	142.6	1785	1793
						1.178	146.8*[g]	1800	
			2(2)	−80 (43)	29	1.173	137.2	1780	1776
						1.174	137.9*	1772	
		2Al-*meta*[h] (2)	2(1)	−98 (66)	38	1.178	141.4	1761	1767
						1.177	146.1*	1774	
			2(2)	−90 (40)	34	1.176	135.9	1754	1758
						1.178	137.8*	1762	
		2Al-*para* (1)	2(2)	−81 (46)	30	1.175	139.9	1774	1780
						1.172	139.6*	1785	
	site III	2Al	2(2)	−169 (4)	98	1.175	145.1	1789 (1796)[i]	1789
Y2	site II	1Al (1)	2(1)	−80 (81)	29	1.174	142.0	1785	1793
						1.172	146.5*	1801	
			2(2)	−79 (43)	29	1.173	136.8	1782	1784
						1.172	138.5*	1785	
		2Al-*meta* (1)	2(2)	−80 (43)	29	1.177	130.3	1767	1774
						1.173	138.3*	1778	
						1.179	134.7*	1743	
X	site II	3Al (2)	2(1)	−73 (88)	26	1.180	135.6	1749	1758
						1.183	133.8*	1766	
			3(3)	−79 (45)	29	1.180	141.4	1739	1729
						1.178	147.0*	1718	

^{a} nAl: For site II clusters denotes number of Al atoms within the 6T ring; value in parentheses refers to number of Al atoms in the remaining part of the QM cluster. For site III clusters denotes the total number of Al atoms in QM cluster. ^{b} Cu coordination number to framework O atoms. $m(n)$: m denotes total Cu−O coordination number; n number of distinct coordinated TO$_4$ units. ^{c} See text for definition. ^{d} Calculated according to the eq 3. ^{e} See text for clarification. ^{f} See text for detailed description of various "Y lattice" models. ^{g} Star depicts Cu−N−O species bent toward the plane of the 6T ring. ^{h} *Meta* and *para* denote mutual Al atom positions in the 6T ring. ^{i} Value obtained for 20T QM cluster.

for these sites are about 80 kJ/mol, while for 6T/1Al and 6T/2Al rings with 2(2) coordination, the numbers approach 50% of appropriate adsorption energies. A similar trend is found 6T/3Al rings with 2(1) and 3(3) Cu(I) coordination.

Structural and Energetic Properties of Dinitrosyl Species. A variety of dinitrosyl structures, being the local minima on the potential energy surface, have been found in the optimization process, depending on the initial geometry (see Figure 8). Due to the radical nature of NO, structures with the second NO molecule adsorbed on the first one and not bound directly to Cu(I) are also possible. In some cases, stable complexes with a Cu−NO−NO−extralattice H bridge have been found. This

indicates that dinitrosyl species bridging two Cu(I) ions may also be possible in Cu(I)FAU zeolites, which are beyond the scope of our "single Cu(I)" models. Nevertheless, the most stable dinitrosyl species are those with both NO molecules bound directly to the Cu(I) ion via nitrogen and close to the parallel alignment of adsorbed molecules. Selected results for dinitrosyls are presented in Table 3, see also Figures 6 and 7. More information is included in Supporting Information.

For given types of dinitrosyl complexes, similar structures have been found for singlet and triplet states, with the distance between O atoms belonging to both ligand molecules about 0.4 Å shorter and Cu−N−O angles about 10° less obtuse for the

NO Interaction with Cu(I) Sites in Zeolites X and Y
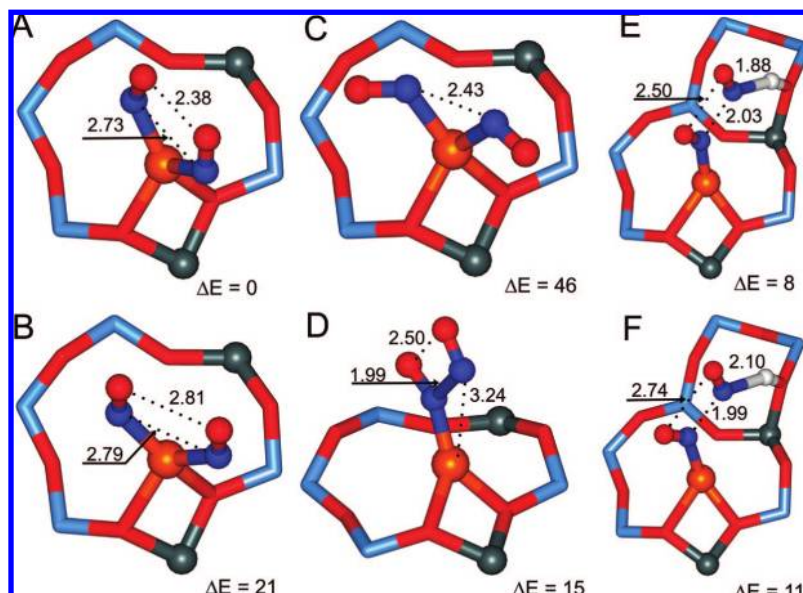
J. Phys. Chem. C, Vol. 112, No. 46, 2008 **18005**

Figure 8. Selected possible dinitrosyl species in site II with two Al atoms in *meta* positions (Y1 model), fragments of optimized QMPot structures: (A, C−E) singlet states; (B, F) triplet states. Relative stabilities, ΔE, are given in kJ/mol, with the most stable (panel A) structure taken as the reference level. Cu, Al, and H atoms and NO molecules are depicted with balls. The most important interatomic distances are given in Å.

TABLE 3: Properties of the Dinitrosyl Species Calculated for Y and X Zeolite Models for Singlet States, Structural Parameters (Distances in Å, Angles in deg), Interaction Energies (kJ/mol), and NO Stretching Bond Harmonic Frequencies (cm^{-1})

model	Cu(I) site	nAl[a]	CN$_{Cu}$[b]	R_{Cu-N}	R_{N-O}	R_{O-O}[d]	R_{N-N}	θ_{Cu-N-O}	E_{ads} (E_{def})[e]	ΔH_{ads}[f]	ω_{NO}[c]
Y1[g]	site II	1Al	2(1)	1.886	1.167	2.37	2.72	127.7	−74 to −79[h]	34 to 37	1694
		(2)		1.966	1.164			124.9	(94)		1816
		2Al-*meta*[i]	2(1)	1.875	1.174	2.38	2.73	127.6	−72 to −80	33 to 38	1676
		(2)		1.979	1.161			124.4	(80)		1809
		2Al-*para*	2(2)	1.932	1.170	2.38	2.73	125.7	−73(75)	34	1684
		(2)		1.958	1.162			125.3			1807
	site III	2Al	2(1)	1.903	1.168	2.39	2.73	126.3	−87(5)	42	1690 (1695)
				1.920	1.167			125.6			1810 (1816)
Y2	site II	1Al	2(2)	1.958	1.165	2.36	2.71	124.5	−66 to −68	30 to 31	1697
		(1)		1.960	1.162			124.5	(85)		1821
		2Al-*meta*	2(2)	1.932	1.162	2.37	2.71	125.4	−68	31	1679
		(1)		1.983	1.171			123.5	(76)		1807
		2Al-*para*	2(2)	1.964	1.175	2.38	2.80	123.5	−74	34	1670
		(1)		2.012	1.159			122.4	(81)		1800
X	site II	3Al	2(2)	1.934	1.165	2.38	2.69	124.7	−68	31	1663
		(2)		2.034	1.173			122.1	(78)		1787

[a] nAl: For site II clusters denotes number of Al atoms within the 6T ring; value in parentheses refers to number of Al atoms in the remaining part of the QM cluster. For site III cluster is total number of Al atoms in the QM cluster. [b] Cu coordination number to framework O atoms. $m(n)$: m denotes total Cu−O coordination number; n denotes number of distinct coordinated TO$_4$ units. [c] Only Cu−O distances closer than 2.5 Å are considered. [d] Distances between atoms belonging to NO molecules. [e] See text for definition. [f] Calculated according to the eq 3 with f taken from MP2 and CASPT2 calculations. [g] See text for detailed description of various "Y lattice" models. [h] Range depends on the energy of initial mononitrosyl species (see Table 2) applied in formula 1. [i] *Meta* and *para* denote mutual Al atom positions in 6T rings.

TABLE 4: Comparison of the Second and First NO Binding Energies (kJ/mol) Obtained with Various Computational Methods for Cu(I)−Al(OH)$_4$ Cluster Model[a]

	E_{ads}	
method	first NO	second NO
DFT/PBE	−178	−72
DFT/B3LYP	−120	11
MP2	−145	−52
CASPT2 (π NO not active)	−120	−34
CASPT2 (π NO active)	−103	

[a] All values are BSSE corrected.

singlets. The second NO molecule is bound about 10 kJ/mol more strongly in the singlet state than for the corresponding triplet complex. This additional stabilization energy comes

mainly from the bond formation between the adsorbed NO molecules. Differences in the heats of the second NO molecule adsorption between sites III and II are rather small, with a few kilojoules per mole preference for site III.

It has been noted that at DFT level, PBE functional predicts the binding of the second NO molecule while B3LYP gives the second energy of adsorption close to zero or even positive, in qualitative contradiction with experiment. To resolve this ambiguity, some calibrating calculations were performed for cluster models (NO)$_{0-2}$−Cu(I)AlO$_4$, employing DFT (PBE and B3LYP functionals) and wave function based (MP2 and CASPT2) methods. Only singlet states were considered. The active space for CASPT2 was composed of five 3d orbitals of Cu plus corresponding 4d double-shell orbitals (with 4s admixture), supplemented with π^* and π orbitals of NO.

18006 *J. Phys. Chem. C, Vol. 112, No. 46, 2008*

Rejmak et al.

However, for the dinitrosyl complex, this choice would lead to 18 active orbitals (which is beyond present computational capabilities); therefore the smaller active space without the π orbitals of NO was also considered. All binding energies were corrected for basis set superposition error. The results are given in Table 4.

The DFT results for the model systems (with the stress on the difference between PBE and B3LYP) are analogous to the results obtained for bigger clusters. For the first binding energy, the B3LYP functional yields similar results as CASPT2, about 0.58−0.67 of the PBE result. MP2 predicts somehow higher binding energy, about 0.81 of the PBE result. For the second binding energy, B3LYP completely fails, while PBE functional performs qualitatively correctly. However, PBE once again overestimates the binding energy in comparison to MP2 and CASPT2. The latter methods yield 0.72 and 0.47 of the PBE second binding energy, respectively. Because it is hardly possible to decide which of these two is more accurate (the NO π orbital was inactive in the CASPT2), we conclude to use here the average value (0.6) as the approximate scaling factor for the second NO adsorption energy in eq 3.

The multireference character of the CASSCF wave function is strongly pronounced for dinitrosyls due to the weak bond between two NO molecules, arising from the σ-type overlap between the π* orbitals. The natural occupation numbers for the bonding and antibonding combination are 1.6 and 0.4 (instead of 2 and 0), respectively, indicating that the bond is partially broken already at the equilibrium geometry. For the cases of strong static correlation, it was suggested that pure functionals (like PBE) might be better suited than the hybrid functionals (like B3LYP),[58] which may explain the failure of B3LYP in our case.

Deformation energies for dinitrosyls are close to the values calculated for the corresponding mononitrosyl forms in the case of site III and site II with 2(1) Cu(I) coordination. Again the HS model predicts 2(1) Cu(I) coordination for all adsorption complexes in site II and additionally stable dinitrosyl complexes with 3(3)-coordinated copper for the 6T/3Al ring. High-alumina models (Y1, Y2, and X) predict 2(1), 2(2), and even 1(1) Cu(I) coordination for 6T/1Al rings, 2(1) and 2(2) for 6T/2Al rings, and 2(2) for 6T/3Al ones. Cu−N bonds are bout 0.1 Å elongated, NO bonds about 0.05 Å shorter, and Cu−N−O angles about 15°−20° smaller than the corresponding values in mononitrosyl species.

Vibrational Analysis. Harmonic vibrational analysis is performed for the majority of the predicted structures, both to confirm that the found stationary points are true minima and to help in the interpretation of IR spectra of adsorbed NO molecules. No imaginary modes in QMPot frequencies are found. Stretching modes of NO molecules adsorbed on site III are essentially the same irrespective of the number of Al and H atoms in the vicinity of the Cu(I), and type of Cu(I) siting (wave numbers are about 1785 and 1800 cm^{-1} for small 8T and larger 20−22T clusters, respectively). Mononitrosyl species in site II show a decrease in NO frequency with increase of Al content in the 6T ring and increase in the number of TO$_4$ units connected to the Cu(I) cation. Stretching NO frequencies calculated for the nitrosyl species bent toward and out of the plane of the 6T ring differ typically by about 10 cm^{-1}, but it can be assumed that the observed frequency is averaged due to nearly free rotation along the Cu−N axis. Because nitrosyl complexes bent "toward" and "out of" the plane have the same energy and intensities of given modes are very similar, we simply take the arithmetic average of both frequencies as the effective one (the

last columns in the Tables 1 and 2). Frequencies defined in this way lie in the range 1793−1729 cm^{-1} and decrease in the series: 1Al-2(1) > 1Al-2(2) ≥ 2Al-2(1) > 2Al-2(2) ≥ 3Al-2(1) > 3Al-3(3), where nAl-$m(p)$ denotes the number of Al in the 6T ring and the Cu coordination.

Frequencies of the dinitrosyl species are less site specific than those of the mononitrosyl ones. Calculated values for the dinitrosyl species in site II cover densely the ranges 1663−1697 and 1791−1829 cm^{-1} for asymmetric and symmetric modes, respectively. Still some decrease in frequency with the number of Al atoms in the 6T ring can be found for site II but less pronounced than that for the mononitrosyl species. Final Cu(I) coordination does not seem to affect vibrational modes. Frequencies of the corresponding singlet and triplets states differ usually by less than 10 cm^{-1}, so even if the triplet states are present in FAU, they should be hardly distinguishable by IR spectroscopy.

5. Discussion

Computational results obtained for models containing 6T/1Al and 6T/2Al rings may be regarded as representative for Cu(I)Y, while models with 6T/3Al rings represent higher alumina Cu(I)X with respect to Al loading in different kinds of FAU. Less-stable site III can be expected to be occupied by Cu(I) in high-alumina X zeolite, if occupied at all. Consequently, when discussing Cu(I) sites in FAU, we mean Cu(I) in site II, if not stated otherwise. The computational part of this study deals only with isolated Cu(I) species. Particularly in highly exchanged Cu(I)X, interactions between copper sites are very likely and can affect adsorption properties of this system. We hope, however, that our conclusions are well-supported for Cu(I)Y, where distances between copper ions are rather large. Nevertheless, even for Cu(I)X, the inspection of isolated copper species is necessary prior to studying more sophisticated (i.e., "multi-Cu(I)") models in the future. As we will show in this section, reasonable explanation of the available experimental data can be accomplished on the basis of the results obtained for isolated Cu(I) species. However, we do not claim that the interpretation given in this section is ultimate. The summary of the experimental and computational results is given in Table 5.

Structures and Energetics. Previous QMPot studies on Cu(I) centers showed monovalent copper in FAU favoring planar trigonal coordination.[49] Such coordination to framework O atoms is less likely in zeolites with strongly distorted lattice structure, like MFI.[36] Therefore Cu(I) sites in MFI may strongly interact with adsorbing molecules to form adsorption complexes with favorable 3-fold planar coordination to two lattice O atoms and to one ligand atom.[28,59,60] Contrary to MFI, the Cu(I) ion in the more symmetrical FAU lattice can easily adopt the preferable planar 3-fold coordination to O atoms (the 6T ring has approximate *C*3 symmetry) and is not apt to leave this position. Thus the heats of NO adsorption predicted here on Cu(I) in position II (30−40 kJ/mol) are much smaller than values for Cu(I)MFI and are closer though still below the values calculated for flat hexagonal rings in FER.[28] Very low heat of NO adsorption on Cu(I) in site II is one of the most apparent calculated properties. Unfortunately, we have not found any microcalorimetric data to support this prediction. Because of the fine agreement between the previous QMPot studies[28] and experimental ones,[61] we expect that our results are fairly acurate. Site III with Cu(I) connected to two framework O atoms binds ligands much more strongly, and in this case, the calculated heats of adsorption (90−110 kJ/mol) are comparable to the ones obtained for Cu(I) sites in MFI or 2-fold coordinated Cu(I) in

TABLE 5: Summary of the Experimental and Theoretical Results, The Predicted Properties of Cu(I)−(NO)$_{1-2}$ Species for Cu(I) Coordination (CN$_{Cu}$), NO Adsorption Heats (ΔH$_{ads}$), and Harmonic Frequencies (ω$_{calcd}$) in the Various Types of FAU Zeolite, along with the Assignment of Experimental Bands (ν$_{exp}$)^a

zeolite type	Cu(I) siting	mononitrosyls				dinitrosyls			
		CN$_{Cu}$^{b}	ω$_{calcd}$	ν$_{exp}$	ΔH$_{ads}$	CN$_{Cu}$	ω$_{calcd}$	ν$_{exp}$	ΔH$_{ads}$
US-Y	site II 6T/1Al	2(1)	1790	1815	50	2(1)	1690 1815	1730	30
Y	site II 6T/1Al	2(1)	1790	1815	30−40	2(1)	1695 1820		25−30
		2(2)	1775−1785	1793		2(1)	1670−1680	1730 1825	
	site II 6T/2Al	2(1)	1760−1775			2(2)	1810		
		2(2)	1755−1775	1780					
X	site II 6T/2Al	2(1)	1760	1772	30	2(1)	1675 1800		20
			1730−1740	1757		2(2)	1645−1665	1700 1820	
						3(3)	1790−1795		
	site III	2(1−2)	1795−1805		90−110	2(1)	1695−1700		30−35
							1815−1825		

^{a} Heats in kJ/mol; frequencies in cm^{-1}. ^{b} Cu coordination number to framework O atoms. $m(n)$: m denotes total Cu−O coordination number; n denotes number of distinct coordinated TO$_4$ units.

FER.[28] Subspecies of site III with 2(1) coordination adsorb NO about 20 kJ/mol more strongly than the ones with 2(2) coordination (see Figure 7).

To achieve the favored planar 3-fold coordination upon NO adsorption, Cu(I) species connected to three framework O atoms must either break one of the bonds and create a new one (in the case of 3(2) coordination) or break two bonds and create two new ones (in the case of 3(3) coordination). The former situation occurs in MFI and FER[28] (see Figure 6D), the latter one in FAU (see Figure 6A,B,C). Less-stable Cu(I) species coordinated only to two O atoms bind the ligand without significant change in their siting. The smaller the distortion in Cu(I) siting upon the ligand adsorption, the larger the heat of adsorption is and, by definition, the smaller the deformation energy is. Our study shows that in the case of NO adsorption both structures with 2(1) and structures with less-distorted 2(2) coordination are possible. Both forms are equally probable energetically, but due to much smaller deformation, the adsorption complexes with 2(2) coordination can be tentatively suggested to be kinetically favored. Only for 6T/3Al rings, where Cu(I) stabilization is the strongest,[49] structures with 3(3) coordination preserved after NO adsorption are slightly more stable than those with 2(1) coordination. The displacement of Cu(I) due to adsorption has been observed experimentally[19] and shown by theoretical studies on Cu(I) sites in zeolites.[28,49,59] The decrease in the NO binding strength with the increase of number of Al atoms inside the 6T ring predicted by the HS model is not confirmed by more reliable Y models.

The heats of adsorption for the second NO molecule are very similar for sites II and III (30−40 kJ/mol). This is the result of very similar Cu(I) siting in mononitrosyl complexes in both sites (see Figures 6 and 7). After the first NO molecule adsorption, Cu(I) usually adopts 2(1) or 2(2) coordination, as in site III. Moreover, the adsorption heats for the first and the second NO molecule are almost the same in site II. On the contrary, for site III, the second heats of adsorption are over 2 times smaller than the first ones. This result finely agrees with the observation that in Cu(I)FAU bands of mono- and dinitrosyl species develop almost simultaneously, while in MFI zeolite, which hosts Cu(I) in more "FAU site III like" positions, bands from dinitrosyl appear at higher NO pressure. Indeed, our QMPot calculations done on Cu(I)−dinitrosyl species in MFI (not presented here) show that the second heats of adsorption in this zeolite are about 45 kJ/mol, thus over 2 times smaller than the first heats of NO adsorption on Cu(I)MFI.[28]

IR Spectra. Exact assignment of the observed bands is a difficult task, both due to the mentioned discrepancy in the experimental data and becuase frequencies calculated in this study are the harmonic ones. However, we believe that the errors introduced by the neglected anharmonicity and by some inherent errors of used computational methods should be quite systematic; thus the relative positions of the calculated bands should be comparable to the experimental ones. Calculated here, harmonic DFT/PBE frequencies are smaller than the experimental ones. Scaling factors available in literature, developed for main group compounds, are usually smaller than unity[62] and thus *a priori* cannot improve our results. Inspection of the calculated bond lenghts and stretching frequencies (Tables 1 and 2) shows also that no linear scaling, for example, like that derived for Cu(I)−CO species,[63] can be expected for Cu(I)−NO complexes. Therefore we decided to present the calculated harmonic modes without applying any scaling of fitting procedure.

Three main conclusions follow from the inspection of the calculated harmonic modes of the mononitrosyl species: (i) frequencies decrease with the increase of Al atoms in the 6T ring; (ii) for a given number of Al atoms within the 6T ring, the species with 2(1) copper coordination have higher frequency than those with 2(2) or 3(3) coordination; (iii) frequencies of site III species are higher than those of ones adsorbed on site II and do not vary with the number of Al atoms in the vicinity of Cu(I) ion.

All three mononitrosyl bands observed in Cu(I)Y (1815, 1793, and 1780 cm^{-1}) should be attributed to different subspecies of site II. The highest band (1815 cm^{-1}) has been observed only by Turnes Palomino et al.[19] This band was visible only at low NO pressure, and the peak was of low intensity. A similar band (1815−1819 cm^{-1}) has been observed for Cu(I)USY by Cheung et al. In our theoretical models, the highest NO frequency (1788−1793 cm^{-1}) is always predicted for the mononitrosyl species in 6T/1Al with 2(1) copper coordination. Such mononitrosyl complex with 2(1) copper coordination is the only one found in 6T/1Al ring in HS lattice that can resemble Cu(I) sites in USY zeolite. The lack of this band in the present IR experimental data and in those from ref 9 can be caused for several reasons. Signals from 6T/1Al species are expected to have lower intensity than those from 6T/2Al rings, because the number of 6T/1Al rings is smaller than the amount of 6T/2Al rings in the Y zeolite lattice. In addition Cu(I) is bound more weakly in 6T/1Al rings.[49] As shown in Y models, the mononitrosyl species with 2(1) and 2(2) coordination within 6T/1Al

rings have the same stability, but the latter ones are less distorted from the initial Cu(I) siting and may be favored kinetically. More exposed Cu(I) siting in mononitrosyl species with 2(1) coordination should make the formation of dinitrosyls more probable than in mononitrosyls with 2(2) coordination. All these factors may make observing IR signals from mononitrosyls with 2(1) coordination possible only at very high Cu(I) loading, when overall Cu(I) concentration in 6T/1Al rings is high, and at low NO pressure, when the rate of dinitrosyl formation is low, as in ref 19.

Calculated frequencies for the remaining site II species overlap partially. Based upon the predicted trend, we suggest that the middle band in experimental spectra (1793 cm^{-1}) comes mainly from the mononitrosyl complexes in 6T/1Al rings with 2(2) copper coordination and 6T/2Al rings with 2(1) coordination, while the lowest band is mainly contributed by species in 6T/2Al rings with 2(2) copper coordination. The lowest band at 1780 cm^{-1} is clearly seen only on difference spectra;[54] that is probably why it has not been reported in refs 12 and 19.

Two mononitrosyl bands, 1757 and 1772 cm^{-1}, have been measured in this work for Cu(I)X. The results obtained for the HS model containing the 6T/3Al ring and the X model suggest that both bands can be assigned to site II with three Al atoms in the vicinity of Cu(I) but differing by the final Cu(I) coordination. The higher band should come from species with Cu(I) coordinated to a single AlO$_4$ unit, while the lower band is expected to come from those species with Cu(I) maintaining 3(3) coordination. Stronger intensity of the band assigned to the Cu(I) sites with higher coordination can be again attributed to their kinetically easier formation, due to the smaller Cu(I) distortion.

Lack of the mononitrosyl signals from sites III, apart from their low occupation by Cu(I) ions, can be explained by their easier transformation into the dinitrosyls. Site III species bind the second NO molecule slightly more strongly than site II species with 6T/3Al rings. Also more exposed Cu(I) siting and smaller distortion during the NO adsorption (very small deformation energy) may kinetically favor dinitrosyl formation in these sites. In addition, proximity of the mononitrosyl bands from site III (about 1785 and 1800 cm^{-1} for small and large clusters, respectively) and the dinitrosyl bands, particularly those from site II with 6T/3Al rings (1790−1800 cm^{-1}), may make these signals hardly separable from each other.

Dinitrosyl species do not show clear site-specifity. Observed dinitrosyl bands are difficult to interpret due to strong dependency of their intensities on the angle between the NO molecules (see ref 20 and references therein). Theoretical results are also ambiguous, due to the variety of possible dinitrosyl species of similar stability. Although the general trend predicted for the mononitrosyl species is maintained, that is, the sites characterized by higher modes of mononitrosyl species can be associated with the higher frequencies of dinitrosyl species, it is not so apparent as in the case of mononitrosyls.

General Remarks. The interpretation given above is generally consistent with the previous QMPot study of CO adsorption on Cu(I)FAU.[49] Frequencies of the species adsorbed on site II (CO and NO) decrease with the number of Al atoms. This can be explained by the higher Lewis basicity of the 6T rings containing more Al atoms, which enhances back-donation from 3d Cu(I) orbitals toward the π* orbitals of the ligands. Due to the antibonding character of such orbitals in CO or NO, this results in the bond weakening and lowering stretching frequencies. Site III species are more exposed to the supercage and should experience rather the overall averaged influence of the

lattice; thus their properties do not vary with the Al content in their closest vicinity. The main difference between CO and NO adsorption is the existence of the different nitrosyl species deriving from the same initial bare ion position and varying by the final Cu(I) coordination in adsorption complex. For the strongly adsorbing CO molecule, dominant adsorption species are those with the Cu(I) ion strongly distorted from bare ion siting, usually adopting 2(1) coordination. In the case of the NO molecule, two stable mononitrosyl species are possible within the same type of Cu(I) center, either more or less distorted from the initial Cu(I) siting and characterized by different NO stretching frequencies. Within the presented explanation, the NO molecule can be considered as only "partially site specific" because some bands from different Cu(I) sites, namely, 6T/1Al and 6T/2Al rings, can overlap depending on the final Cu(I) siting achieved in the mononitrosyl complex. On the other hand, different mononitrosyl bands can be derived from the same initial Cu(I) siting when NO adsorption results in two equally stable species differing by the achieved Cu(I) coordination. Mononitrosyl complexes with 2(2) copper coordination are predicted only within Y models. This shows that in some cases long-range influence of the lattice and Al loading may seriously affect the properties of active sites in zeolites and must be considered in theoretical models.

A few remarks should be made on the interpretation proposed by Turnes Palomino et al.[19] They have assigned different bands in Cu(I)Y, both for CO and for NO, to the Cu(I) more or less displaced from the plane of the 6T ring (sites II and II* in their nomenclature, respectively). Such interpretation has been questioned by the theoretical studies. Both QM cluster[64] and QMPot[49] models of Cu(I)FAU have predicted isolated Cu(I) ions siting almost exactly in the plane of the 6T rings. The adsorbing CO molecule strongly displaces the Cu(I) ion; thus small differences in initial copper siting should not influence the final structure and stretching modes of monocarbonyl species. However, it should be noted here that subspecies of site II more exposed to the supercage may be present at high Cu(I) loading, where the other neighboring cation may influence Cu(I) siting. This situation may not be described properly by the "single Cu(I)" theoretical models,[49,64] including the present one. Such Cu(I) species can more likely form mononitrosyl species with 2(1) coordination and subsequently dinitrosyls. However, we conclude that the position of the monitrosyl bands in Cu(I)Y should depend on the number of Al atoms in the 6T rings (as for CO) and final Cu(I) siting, while the factors considered by Turnes Palomino et al. may rather affect the relative intensity of the bands.

Finally, we would like to point out very strong activation of a single NO molecule on Cu(I)-exchanged FAU. Red shift of NO stretching frequency with respect to the gas-phase molecule is about 60 cm^{-1} for mononitrosyl species in majority of Cu(I) zeolites,[20] while it is 60−110 cm^{-1} for Cu(I)FAU. Despite this fact, the rate of direct NO decomposition on Cu(I)Y is 1 order of magnitude lower than that on Cu(I)MFI with much lower Cu(I) loading.[65] Few factors can contribute to such behavior. First, about one-half of Cu(I) ions introduced in FAU occupy sites inside the hexagonal prisms, not accessible for adsorbing molecules.[19] Second, the heats of single NO molecule adsorption are more than 2 times lower in Cu(I)FAU than in Cu(I)MFI; thus slower NO adsorption can limit the ratio of the overall process. It is often postulated that NO decomposition proceeds via some dinitrosyl species.[11,27,66,67] In such a case, stronger activation of a single NO molecule would not control the deNOx activity of a given zeolite. It would be interesting to compare

the results of the catalytic tests on NO decomposition on Cu(I)X; however, as far as we know, they are not available in literature.

6. Conclusions

NO adsorption on Cu(I)FAU has been investigated by combined means of IR spectroscopy and theoretical QM/MM modeling. Contrary to other Cu(I) zeolites, few mononitrosyls bands are observed in Cu(I)FAU. Mononitrosyl bands are more red-shifted than in other zeolites, but despite stronger activation of a single NO molecule, Cu(I)FAU have been reported as less active in NO decomposition. All mononitrosyls bands can be attributed to Cu(I) sites with the cation coordinated initially to three framework oxygen atoms (site II). The NO stretching frequency is more red-shifted for Cu(I) species with (i) a higher number of Al atoms in their vicinity and (ii) less distorted structure imposed by the binding of NO molecule. No mononitrosyl bands can be attributed to Cu(I) sites with 2-fold coordination to framework O atoms (site III), presumably due to both their lower occupancy and stronger affinity to dinitrosyl species. Predicted heats of NO adsorption are significantly lower than those found for high-silica zeolites, which may be a factor responsible for low deNOx activity of Cu(I)-exchanged FAU.

Supporting Information Available: Geometric parameters of Cu(I) sites before and after single NO molecule adsorption in high silica model, geometric parameters of Cu(I) sites before and after single NO molecule adsorption in Y models, and properties of the dinitrosyl species calculated for high-silica FAU model. This material is available free of charge via the Internet at http://pubs.acs.org.

References and Notes

(1) (a) Iwamoto, M.; Yokoo, S.; Sakai, K.; Kagawa, S. *J. Chem. Soc., Faraday Trans. 1* **1981**, *77*, 1629. (b) Iwamoto, M.; Furukawa, H.; Mine, Y.; Uemura, F.; Mikuriya, S.; Kagawa, S. *J. Chem. Soc., Chem. Commun.* **1986**, 1272.

(2) Hidenori, Y.; Iwamoto, M. *Appl. Catal., A* **2001**, *222*, 163.

(3) (a) Ritscher, J. S.; Sandner, S. U.S. Patent 4,297,328, 1981. (b) Iwamoto, M.; Yahiro, H.; Yu-u, Y.; Shundo, S.; Mizuno, N. *Shokubai* **1990**, *32*, 430. (c) Held, W.; Konig, A.; Richter, T.; Puppe, L. *Soc. Automot. Eng.* **1990**, 900496.

(4) (a) Mizumoto, M.; Yamazoe, N.; Seiyama, T. *J. Catal.* **1979**, *59*, 319. (b) Kieger, S.; Delahay, G.; Coq, B.; Neveu, B. *J. Catal.* **1999**, *183*, 267. (c) Kieger, S.; Delahay, G.; Coq, B.; Neveu, B. *J. Catal.* **1999**, *183*, 267.

(5) Berthomieu, D.; Delahay, G. *Catal. Rev.* **2006**, *48*, 269.

(6) (a) King, S. T. *J. Catal.* **1996**, *161*, 530. (b) Anderson, S. A.; Root, T. W. *J. Catal.* **2003**, *217*, 396. (c) Richter, M.; Fait, M. J. G.; Eckelt, R.; Schreier, E.; Schneider, M.; Pohl, M.-M.; Fricke, R. *Appl. Catal., B* **2007**, *73*, 269.

(7) (a) Takahashi, A.; Yang, R. T.; Munson, C. L.; Chinn, D. *Langmuir* **2001**, *17*, 8405. (b) Hernandez-Maldonado, A. J.; Yang, R. T. *Catal. Rev.* **2004**, *46*, 111.

(8) Iwamoto, M.; Yahiro, H.; Mizuno, N.; Zhang, W.-X.; Mone, Y.; Furukawa, H.; Kagawa, S. *J. Phys. Chem.* **1992**, *96*, 9360.

(9) Valyon, J.; Hall, W. K. *J. Phys. Chem.* **1993**, *97*, 7054.

(10) Liu, D.-J.; Robota, H. J. *Catal. Lett.* **1993**, *21*, 291.

(11) Aylor, A. W.; Larsen, C. L.; Reimer, A.; Bell, A. T. *J. Catal.* **1995**, *157*, 592.

(12) Valyon, J.; Hall, W. K. *J. Phys. Chem.* **1993**, *97*, 1204.

(13) Hoost, T.; Laframboise, K.; Otto, K. *Appl. Catal., B* **1995**, *7*, 79.

(14) Cheung, T.; Bhargava, S. K.; Hobday, M.; Foger, K. *J. Catal.* **1996**, *158*, 301.

(15) Wichterlova, B.; Sobalik, Z.; Dedecek, J. *Catal. Today* **1997**, *38*, 199.

(16) Broclawik, E.; Datka, J.; Gil, B.; Piskorz, W.; Kozyra, P. *Top. Catal.* **2000**, 335.

(17) Lamberti, C.; Bordiga, S.; Salvalaggio, M.; Spoto, G.; Zecchina, A.; Vlaic, G.; Bellatreccia, M. *J. Phys. Chem. B* **1997**, *101*, 344.

(18) Turnes Palomino, G.; Zecchina, A.; Giamello, E.; Fisciaro, P.; Berlier, G.; Lamberti, C.; Bordiga, S. *Stud. Surf. Sci. Catal.* **2000**, *130*, 2915.

(19) Turnes Palomino, G.; Bordiga, S.; Zecchina, A.; Marra, G. L.; Lamberti, C. *J. Phys. Chem. B* **2000**, *104*, 8641.

(20) Hadjivanov, K. I. *Catal. Rev. Sci. Eng.* **2000**, *42* (1−2), 71.

(21) Yokomichi, Y.; Yamabe, T.; Ohtsuka, H.; Kakumato, T. *J. Phys. Chem. B* **1996**, *100*, 14424.

(22) Trout, B. L.; Chakraborty, A. K.; Bell, A. T. *J. Phys. Chem.* **1996**, *100*, 17582.

(23) (a) Schneider, W. F.; Hass, C. K.; Ramprasad, R.; Adams, J. B. *J. Phys. Chem. B* **1997**, *101*, 4353. (b) Ramprasad, R.; Hass, C. K.; Schneider, W. F.; Adams, J. B. *J. Phys. Chem. B* **1997**, *101*, 6903. (c) Schneider, W. F.; Hass, C. K.; Ramprasad, R.; Adams, J. B. *J. Phys. Chem. B* **1998**, *102*, 3692.

(24) Tajima, J.; Hashimoto, M.; Toyama, F.; El-Nahas, A. M.; Hirao, K. *Phys. Chem. Chem. Phys.* **1999**, *1*, 3823.

(25) (a) Solans-Monfort, X.; Branchadell, V.; Sodupe, M. *J. Phys. Chem. A* **2000**, *104*, 3225. (b) Solans-Monfort, X.; Branchadell, V.; Sodupe, M. *J. Phys. Chem. B* **2002**, *106*, 1372.

(26) Pietrzyk, P.; Piskorz, W.; Sojka, Z.; Broclawik, E. *J. Phys. Chem. B* **2003**, *107*, 6105.

(27) Pietrzyk, P.; Gil, B.; Sojka, Z. *Catal. Today* **2007**, *126*, 103.

(28) Davidová, M.; Nachtigallová, D.; Nachtigall, P.; Sauer, J. *J. Phys. Chem. B* **2004**, *108*, 13674.

(29) (a) Eichler, U.; Kölmel, C. M.; Sauer, J. *J. Comput. Chem.* **1997**, *18*, 463. (b) Sauer, J.; Sierka, M. *J. Comput. Chem.* **2000**, *21*, 1470.

(30) Sierka, M.; Sauer, J. *J. Chem. Phys.* **2000**, *112*, 6983.

(31) Sierka, M.; Sauer, J. In *The Handbook of Materials Modelling*; Yip, S., Ed.; Springer: Dordrecht, The Netherlands, 2005; p 241.

(32) Ahlrichs, R.; Bär, M.; Häser, M.; Horn, H.; Kölmel, C. M. *Chem. Phys. Lett.* **1989**, *162*, 165.

(33) Gale, J. D. *J. Chem. Soc., Faraday Trans.* **1997**, *93*, 629.

(34) Dick, B. G.; Overhauser, A. *Phys. Rev.* **1958**, *112*, 90.

(35) Sierka, M.; Sauer, J. *Faraday Discuss.* **1997**, *106*, 41.

(36) Nachtigallová, D.; Nachtigall, P.; Sierka, M.; Sauer, J. *Phys. Chem. Chem. Phys.* **1999**, *1*, 2019.

(37) Rappe, A. K.; Casewit, C. J.; Colwell, K. S.; Goddard, W. A.; Skiff, W. M. *J. Am. Chem. Soc.* **1992**, *114*, 10024.

(38) Perdew, J. P.; Burke, K.; Ernzerhof, M. *Phys. Rev. Lett.* **1996**, *77*, 3865.

(39) Schäfer, A.; Huber, C.; Ahlrichs, R. *J. Chem. Phys.* **1994**, *100*, 5829.

(40) (a) Becke, A. D. *Phys. Rev. A* **1988**, *38*, 3098. (b) Lee, C.; Yang, W.; Parr, R. G. *Phys. Rev. B* **1998**, *37*, 785. (c) Becke, A. D. *J. Chem. Phys.* **1993**, *98*, 1372.

(41) (a) Eichkorn, K.; Treutler, O.; Öhm, H.; Häser, M.; Ahlrichs, R. *Chem. Phys. Lett.* **1995**, *240*, 283; *242*, 652. (b) Eichkorn, K.; Weigend, F.; Treutler, O.; Ahlrichs, R. *Theor. Chem. Acc.* **1997**, *97*, 119. (c) Sierka, M.; Hogekamp, A.; Ahlrichs, R. *J. Chem. Phys.* **2003**, *118*, 9136.

(42) (a) Roos, B. O.; Taylor, P. R.; Siegbahn, P. E. M. *Chem. Phys.* **1980**, *48*, 157. (b) Andersson, K.; Malmqvist, P.-Å.; Roos, B. O. *J. Chem. Phys.* **1991**, *96*, 1218.

(43) Karlström, G.; Lindh, R.; Malmqvist, P.-Å.; Roos, B. O.; Ryde, U.; Veryazov, V.; Widmark, P.-O.; Cossi, M.; Schimmelpfennig, B.; Neogrady, P.; Seijo, L. *Comput. Mater. Sci.* **2003**, *28*, 222.

(44) Reiher, M.; Wolf, A. *J. Chem. Phys.* **2004**, *121*, 10945.

(45) Roos, B. O.; Lindh, R.; Malmqvist, P.-Å.; Veryazov, V.; Widmark, P.-O. *J. Phys. Chem. A* **2005**, *109*, 6575.

(46) Pierloot, K.; Dumez, B.; Widmark, P.-O.; Roos, B. O. *Theor. Chim. Acta* **1995**, *90*, 87.

(47) Smith, J. V. *Adv. Chem. Ser.* **1971**, *101*, 171.

(48) Fowkes, A. J.; Ibberson, R. M.; Rosseinsky, M. J. *Chem. Mater.* **2002**, *14*, 590.

(49) Rejmak, P.; Sierka, M.; Sauer, J. *Phys. Chem. Chem. Phys.* **2007**, *9*, 5446.

(50) Baerlocher, Ch.; Meier, W. M.; Olson, D. *Atlas of Zeolite Framework Types*, 5th ed.; Elsevier: Amsterdam, 2001.

(51) Loewenstein, W. *Am. Mineral.* **1954**, *39*, 92.

(52) Datka, J.; Kozyra, P.; Kukulska-Zajac, E.; Szutiak, M.; Kumar, N. In *Proceedings of the 14th International Zeolite Conference*; van Steen, E. W. J., Callanan, L. H., Claeys, M., O'Connor, C. T., Eds.; Elsevier, 2004; p 1655.

(53) Kukulska-Zajac, E.; Datka, J. *J. Phys. Chem C* **2007**, *11*, 3471.

(54) By the difference spectra, we mean the ones defined by the two consecutive portions of NO, not simply the regular difference between the spectra of zeolites with and without adsorbed NO.

(55) Datka, J.; Kozyra, P. *J. Mol. Struct.* **2005**, *991*, 744–747.

(56) Bludský, O.; Šilhan, M.; Nachtigall, P.; Bucko, T.; Benco, L.; Hafner, J. *J. Phys. Chem B* **2005**, *109*, 3471.

(57) Boys, S. F.; Bernardi, F. *Mol. Phys.* **1970**, *19*, 553.

(58) Harvey, J. N. *Annu. Rep. Prog. Chem., Sect. C: Phys. Chem.* **2006**, *102*, 203.

(59) Nachtigall, P.; Davidová, M.; Šilhan, M.; Nachtigallová, D. *Stud. Surf. Sci. Catal.* **2002**, *142*, 101.

(60) Davidová, M.; Nachtigallová, D.; Bulánek, R.; Nachtigall, P. *J. Phys. Chem. B* **2003**, *107*, 2327.

(61) Gervasini, A.; Picciau, C.; Auroux, A. *Microporous Mesoporous Mater.* **2000**, *457*, 35–36.

(62) Scott, A. P.; Random, L. *J. Phys. Chem.* **1996**, *100*, 16502.

(63) Bludský, O.; Šilhan, M.; Nachtigallová, D.; Nachtigall, P. *J. Phys. Chem. A* **2003**, *107*, 10381.

(64) Jardillier, N.; Berthomieu, D.; Goursot., D.; Reveles, J. U.; Köster, M. *J. Phys. Chem. B* **2006**, *110*, 18440.

(65) Hall, W. K.; Li, Y. *J. Catal.* **1991**, *129*, 202.

(66) Spoto, G.; Bordiga, S.; Scarano, D.; Zecchina, A. *Catal. Lett.* **1992**, *13*, 39.

(67) Giamello, E.; Murphy, D.; Magnacca, G.; Morterra, C.; Shioya, Y.; Nomura, T.; Anpo, M. *J. Catal.* **1992**, *136*, 510.

JP8042686